# CHAPTER 2:

# MATHEMATICAL MODEL AND OPTIMISATION ALGORITHM

# 2. Mathematical model and optimisation algorithm

In chapter 1 the need for a two-dimensional vehicle dynamic simulation program was motivated. In this chapter the basic mathematical model for a two-dimensional vehicle dynamic simulation is developed. The requirements for this model can be summarised as follows:

i. A single body vehicle with up to four axles must be modelled.
ii. The basic kinematics of the vehicle suspension must be taken into consideration. For this purpose an equivalent trailing arm suspension analysis is to be used.
iii. The suspension is to consist of a spring, damper and bump stop, where all of these component characteristics may be non-linear.
iv. Geometrical input should be a minimum since only the basic geometry of the vehicle and suspension is available during the concept design phase.
v. The vehicle motion is to be simulated over rough terrain and therefore a realistic tyre model, that includes both the effects of tyre stiffness and damping, must be used.

This chapter is concluded with the presentation of the basic principles of the mathematical optimisation approach to design. The properties of the LFOPC optimisation algorithm, which will be used in conjunction with the vehicle model to optimise the suspension system, will also be briefly described.

## 2.1 Six degree of freedom vehicle model

Figure 2.1 shows a schematic of a two-dimensional vehicle body and four axles.

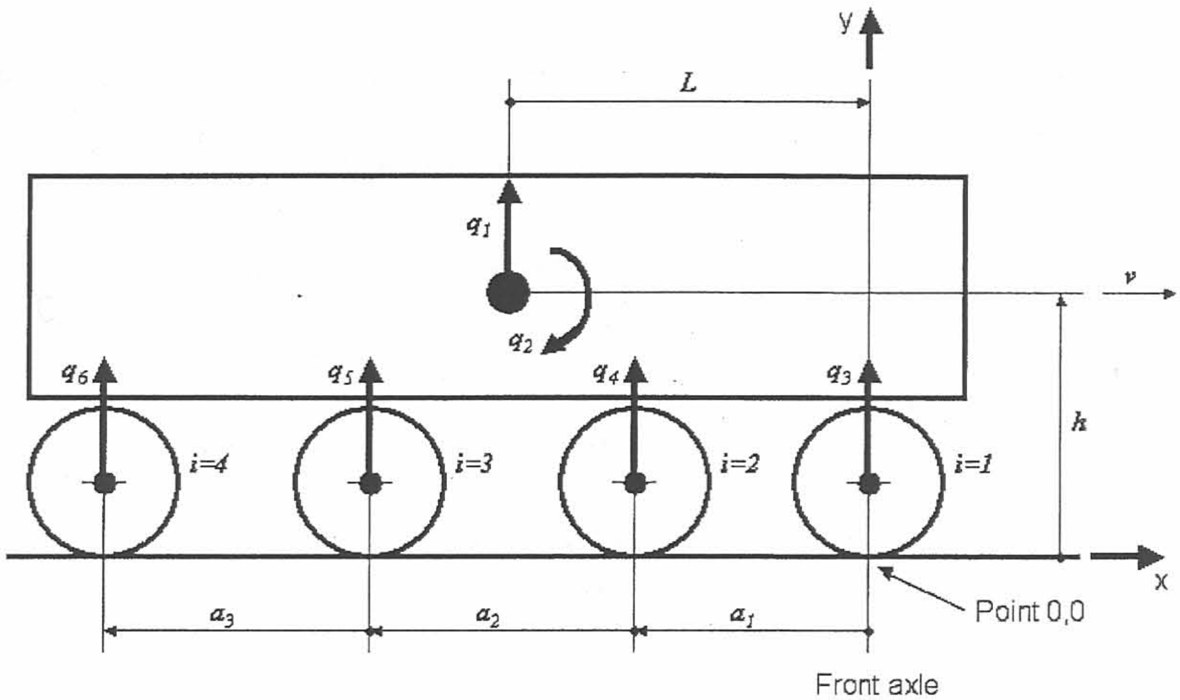


***Figure 2.1: Schematic of the vehicle model (in the initial prescribed position)***

The vehicle system consists of five solid body components, i.e. the vehicle body and four axles. The vehicle body represents the sprung mass and each axle an unsprung mass associated with the specific wheel station $i$. A reference co-ordinate system is defined as the point on the road surface vertically underneath the front wheel centre (point 0,0 in figure 2.1). This is also the reference position for the start of the simulation at time zero specified in seconds by $t = 0$. The initial position of the vehicle at $t = 0$, is the static equilibrium position (or as close as possible to the equilibrium position) and is called the *initial prescribed position* of the vehicle on a level road. The exact equilibrium position will be determined before the simulation starts.

Section A1 of Appendix A gives a complete list of all the parameters and variables used for the vehicle model. A basic description of the model is provided by the following specified parameters (*for the initial prescribed position*):

$m_1$ = mass of the vehicle body (the sprung mass),

$m_{i+1}$ = mass of the unsprung mass associated with each axle $i$, $i = 1,2,3,4$,

$I$ = pitch inertia of the sprung mass about its centre of gravity,

$L$ = horisontal distance between the sprung mass centre of gravity and the centre of the front axle,

$h$ = height of the centre of gravity with respect to the reference point 0,0,

$v$ = horisontal (forward) vehicle speed at the centre of gravity of the vehicle body, and

$a_i$ = distances between axles as indicated in figure 2.1, $i = 1,2,3$.

Six degrees of freedom, measured relative to the *initial prescribed position*, are defined as follows:

$q_1$ = vertical displacement at the centre of gravity of the vehicle body,

$q_2$ = pitch displacement of the vehicle body, and

$q_{i+2}$ = vertical displacement at the wheel centre of axle $i$, $i = 1,2,3,4$.

Displacements are defined as positive vertically upwards and positive pitch displacement indicates a nose down pitch motion of the vehicle. In the initial prescribed position all the degrees of freedom have a value of zero, i.e. $q_i = 0,\ i=1,2,\ldots,6$.

The corresponding velocity values for these six degrees of freedom are denoted by $\dot{q}_i$, $i = 1,2,\ldots,6$, and the associated accelerations by $\ddot{q}_i$, $i = 1,2,\ldots,6$.

The suspension of each of the axles is modelled by an equivalent trailing arm suspension, although the vehicle may not actually be fitted with a trailing arm suspension. In this approximation the axle is connected to a trailing arm that rotates about an axis (at the trailing arm instant centre) that is connected to the vehicle body. More details of this modelling are given in section 3.10. For each axle the total effect of the springs, dampers and bump stops is simulated by an equivalent suspension connecting the centre of the axle vertically upward to the vehicle body. This is shown in figure 2.2, which gives a schematic representation of this model for one of the axles in the *initial prescribed position*.

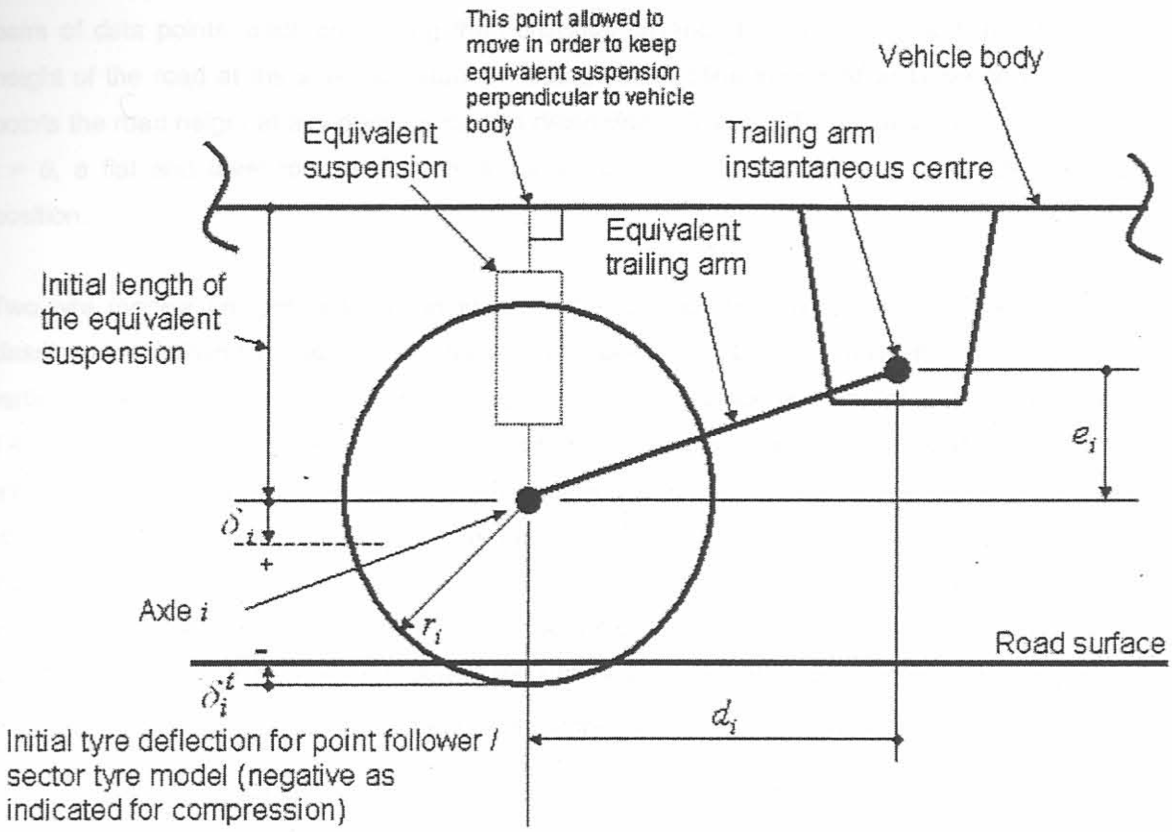


***Figure 2.2: Schematic of the axle showing the equivalent trailing arm and suspension (in the initial prescribed position)***

The following values are assumed known for the model *initial prescribed position*:

$d_i$ = horisontal length of the equivalent trailing arm,

$e_i$ = vertical height of the equivalent trailing arm, and

$r_i$ = rolling radius of the tyre, $i = 1,2,3,4$.

The deflection of the equivalent trailing arm suspension is given by $\delta_i$, $i = 1,2,3,4$ and is determined by the change in the length of the equivalent suspension as shown in figure 2.2. A negative value for $\delta_i$ indicates compression of the equivalent suspension. At the initial prescribed position of the vehicle $\delta_i = 0$, $i=1,2,3,4$. In this position however the actual spring, bump stop and tyre deflection correspond to the initial deflection for these components, namely:

$\delta_i^s$ = initial spring deflection,

$\delta_i^b$ = initial bump stop deflection, and

$\delta_i^t$ = initial tyre deflection, with negative values indicating compression, $i=1,2,3,4$.

The input road profile for the model is given by a discrete two-dimensional data array consisting of pairs of data points, each pair giving the horizontal distance from point 0,0 and the corresponding height of the road at the specific distance. Using cubic spline interpolation between the prescribed points the road height at any distance can be determined. To simplify the calculation of equilibrium at $t = 0$, a flat and level road surface is assumed underneath the wheels at the reference starting position.

Two tyre models are proposed for inclusion in the overall suspension model. The first being the classic point follower model, where the tyre is represented by an equivalent spring and damper, vertically placed between the wheel centre and the road surface and similar to that shown in figure 1.4. This type of tyre model works fine for smooth road surfaces, such as a sinusoidally shaped road with a long wavelength. In instances where the road is rough and the vehicle behaviour for extreme obstacles needs to be simulated, such as for a half round obstacle as shown in figure 2.3, the point follower tyre model does not give realistic results. In such cases the second tyre model, a sector tyre model, should be used. For this sector tyre model the tyre / wheel is divided into a number of sectors and the deflection for each sector, due to the road input, is determined. Finally the deflections of all the sectors are used together to determine respectively the resultant tyre force $f_i^w$ and resultant deflection $\delta_i^w$, $i = 1,2,3,4$. These force and deflection vectors are shown in figure 2.3. Clearly the resultant tyre force is not necessarily vertical as in the case of the point follower, but may be applied at an angle $\varphi_i$, also shown in figure 2.3. The sector tyre model to be used in this study is similar to that used in the more comprehensive vehicle dynamic simulation program GENRIT [3]. The current author developed this model [3] for improved simulation accuracy when using GENRIT. This sector tyre model will not be discussed in detail here.

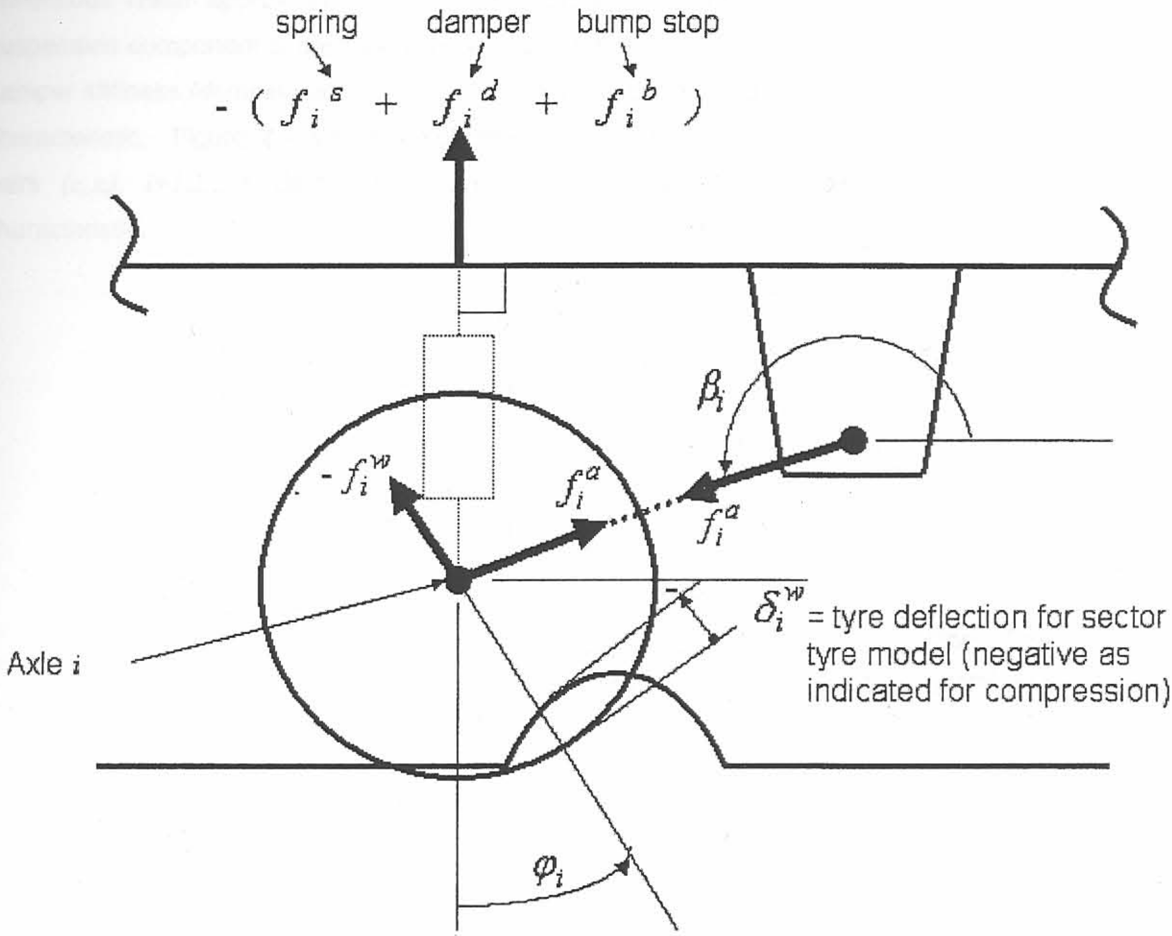


***Figure 2.3: Schematic of the axle showing the road profile and suspension forces***

The suspension forces on the vehicle body (and opposite and equal on the axle) due to each axle $i$, $i = 1,2,3,4$, consist of the following four forces shown in figure 2.3:

| | |
|---|---|
| $f_i^s$ | = equivalent spring force, |
| $f_i^d$ | = equivalent damper force, |
| $f_i^b$ | = equivalent bump stop force, and |
| $f_i^a$ | = force in the equivalent trailing arm. |

The first three forces are defined to be negative for compression (associated with negative deflections), and therefore the upward force on the vehicle is obtained by multiplying their respective values by minus one. The angle $\beta_i$ is the angle of the equivalent trailing arm measured as indicated in figure 2.3

The non-linear characteristics of the suspension and tyres need to be modelled. In order to be able to describe the non-linear force characteristics of these components it was decided to use six piece-wise continuous linear approximations. In this approach the approximation of the characteristic of a suspension component is described by twelve parameters. For example, for a particular damper six damper stiffness (damping coefficient) values and six corresponding deflection rate values define the characteristic. Figure 2.4 shows a schematic for damper characterisation. Clearly the parameter pairs $(c_i, x_i)$, $i=1,2,...,6$ define the piece-wise continuous linear representation of the damper characteristic.

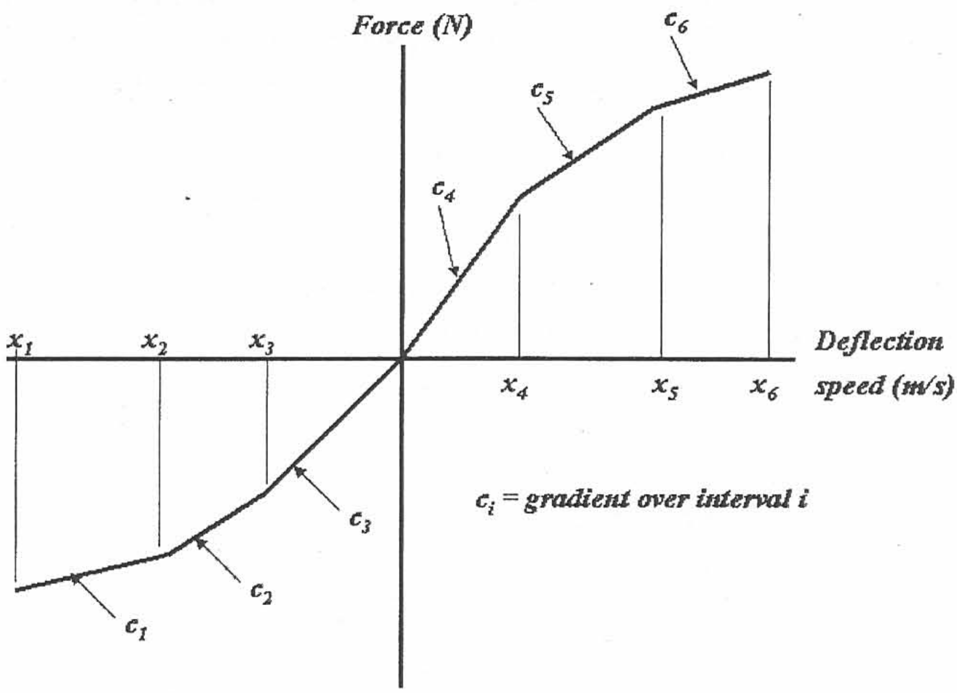


***Figure 2.4: The six piece-wise continuous linear approximation for suspension force characterisation***

Using this six piece-wise linear approximations the damping force, $F$, at any deflection rate $x$, is explicitly and analytically given as follows:

| | | |
|---|---|---|
| For $x < x_2$: | $F = c_3x_2 + c_2(x_2 - x_3) + c_1(x - x_2)$ | (2.1) |
| For $x_2 < x < x_3$: | $F = c_3x_2 + c_2(x - x_3)$ | (2.2) |
| For $x_3 < x < 0$: | $F = c_3x$ | (2.3) |
| For $0 < x < x_4$: | $F = c_4x$ | (2.4) |
| For $x_4 < x < x_5$: | $F = c_4x_4 + c_5(x - x_4)$ | (2.5) |
| For $x > x_5$: | $F = c_4x_4 + c_5(x_5 - x_4) + c_6(x - x_5)$ | (2.6) |

The characteristics for the other suspension components, i.e. for the springs, bump stops and tyres are handled in a similar manner. In the case of spring, tyre and bump stop deflections the data pairs represent the force versus deflection characteristic of the respective components. The deflections used for these components include the initial deflections and the deflections due the equivalent trailing arm deflection (see 2.1.1.2) for more detail.

## 2.1.1 Equations of motion of the vehicle system

Newton's second law can be applied separately to each solid body component of the vehicle system to determine the respective accelerations. The first step in computing the accelerations is to determine all the forces acting on each body at a particular time instant, denoted by the simulation time $t$. At the start of the simulation $t = 0$.

### 2.1.1.1 Tyre forces

In order to determine the wheel forces, the tyre deflections need to be calculated. Figure 2.5 gives a schematic for a part of the vehicle at a particular instant in time. (Note that the angle $\theta$ as indicated in the figure is for negative pitch of the vehicle and is therefore negative. Similarly $\delta_i$ is negative as shown.)

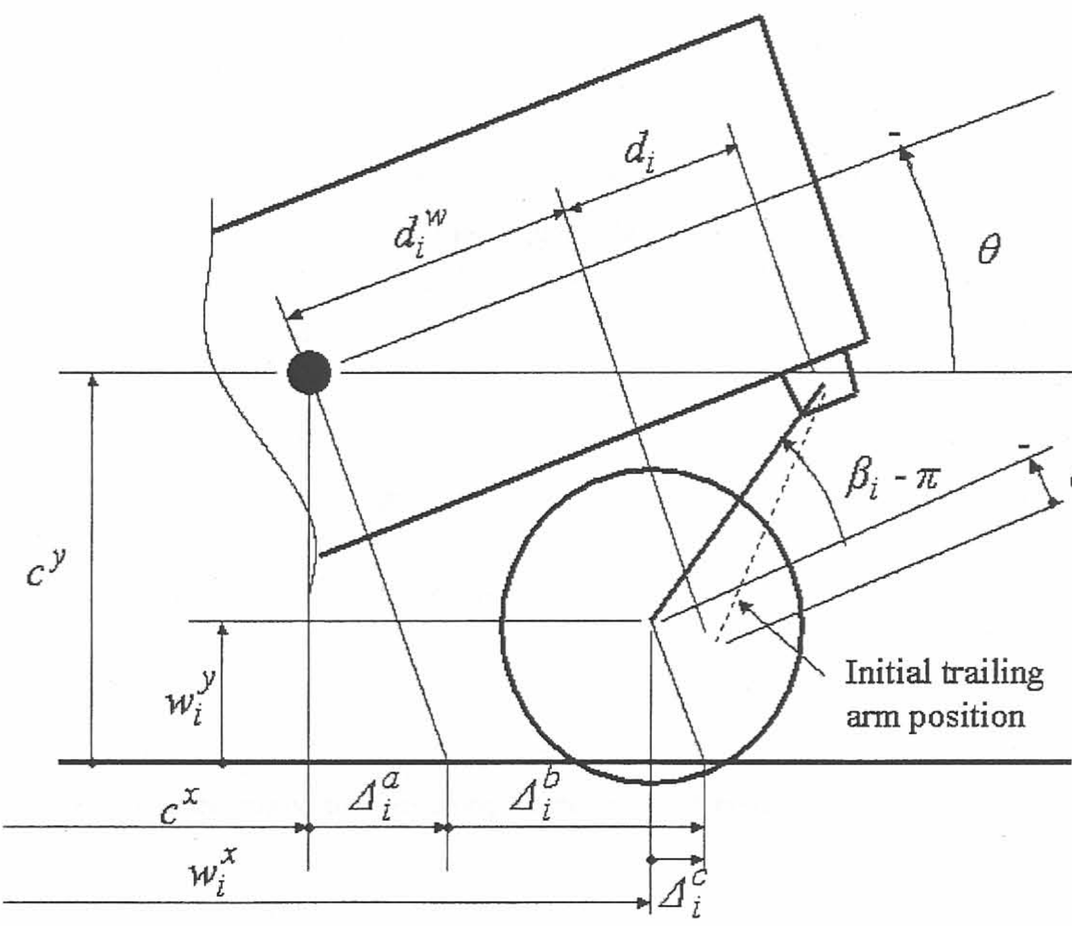


*Figure 2.5: Schematic of a part of the vehicle model showing the parameters used to determine the tyre forces*

The position coordinates relative to the reference point 0,0 shown in figure 2.1, of the centre of gravity of the vehicle are given by:

$$c^y = h + q_1 \tag{2.7}$$

$$c^x = vt - L \tag{2.8}$$

The pitch angle of the vehicle is given by the second degree of freedom:

$$\theta = q_2 \tag{2.9}$$

The longitudinal distance $d_i^w$ between the wheel centre of axle $i$ and the centre of gravity, for the initial prescribed position, is given by

| | | |
|---|---|---|
| for the front axle, $(i = 1)$: | $d_1^w = L$ | (2.10) |
| for the second axle, $(i = 2)$: | $d_2^w = L - a_1$ | (2.11) |
| for the third axle, $(i = 3)$: | $d_3^w = L - (a_1 + a_2)$ | (2.12) |
| for the fourth axle, $(i = 4)$: | $d_3^w = L - (a_1 + a_2 + a_3)$ | (2.13) |

The horisontal position, $w_i^x$ of the wheel centre as measured from the reference point, and the total wheel force $f_i^w$, are obtained via the detailed argument below (up to eq. 2.28).

The vertical height of wheel centre $i$, $i = 1,2,3,4$, is given by:

$$w_i^y = q_{i+2} + r_i + \delta_i^t \tag{2.14}$$

*(remember* $\delta_i^t < 0$ *for tyre compression)*

The length of the equivalent trailing arm is given by:

$$t_i = \sqrt{e_i^2 + d_i^2} \tag{2.15}$$

and the angle $\beta_i$ of the trailing arm (assuming a deflection $\delta_i$ of the equivalent suspension) by:

$$\beta_i = arcsin(\frac{-(e_i + \delta_i)}{t_i}) \tag{2.16}$$

*Note that for a trailing arm suspension $d_i$ is positive and therefore $90° < \beta_i < 270°$, and for leading arm suspension geometry $d_i$ is negative and therefore $-90° < \beta_i < 90°$. The $e_i$ is defined positive if the original wheel centre position is lower than the equivalent trailing arm instantaneous centre.*

The respective lengths $\Delta_i^a$, $\Delta_i^b$ and $\Delta_i^c$ indicated in figure 2.5 are given by:

$$\Delta_i^a = -c^y \tan\theta \tag{2.17}$$

$$\Delta_i^b = \frac{d_i^w + d_i + t_i \cos\beta_i}{\cos\theta} \tag{2.18}$$

$$\Delta_i^c = -w_i^y \tan\theta \tag{2.19}$$

and the distance, $w_i^x$, is therefore given by

$$w_i^x = c^x + \Delta_i^a + \Delta_i^b - \Delta_i^c \tag{2.20}$$

If the sector tyre model is used then, determine the radial tyre deflection $\delta_i^w$ at $(w_i^x, w_i^y)$, the angle for the resultant tyre force $\varphi_i$ and the tyre force factor $\Lambda_i$ using the tyre sector model [3]. The tyre force factor $\Lambda_i$ is a factor that takes the shape of the specific obstacle (that deflects the tyre) into consideration. The tyre stiffness is normally measured for deflection from a flat surface and in this instance $\Lambda_i = 1$. For other shapes of obstacles the factor $\Lambda_i$ is determined by the ratio between the deflection area (in side view) for the specific obstacle, and that obtained for deflection from a flat surface. Normally in these instances $\Lambda_i < 1$.

If the point follower tyre model is used then, determine the height of the road profile $h_i^r$, at $w_i^x$ using cubic spline interpolation of the prescribed road profile data. For this model:

$$\delta_i^w = q_{i+2} - h_i^r + \delta_i^t \tag{2.21}$$

$$\varphi_i = 0 \tag{2.22}$$

$$\Lambda_i = 1 \tag{2.23}$$

The wheel deflection is limited to negative values since the tyres can only experience compression, i.e.:

If $\delta_i^w > 0$ then set $\delta_i^w = 0$ (2.24)

The tyre deflection rates are estimated by backward finite differences:

$$\dot{\delta}_i^w = \frac{\delta_i^w(t) - \delta_i^w(t - \delta^t)}{\delta^t} \qquad (2.25)$$

for $i$, $i = 1,2,3,4$, and where $\delta^t$ is a suitable small time step.

Once the tyre deflections $\delta_i^w, i = 1,2,3,4$ are known, the wheel forces $F_i^{ws}$ can be calculated by using equations 2.1 to 2.6 together with the tyre stiffness/deflection parameters characterising the tyre stiffness. Once $F_i^{ws}$ is known, the wheel force due to tyre stiffness can be determined using the prescribed input for the number of tyres per axle, $n_i^w$, and the tyre factor $\Lambda_i$, calculated by using the tyre sector model or the point follower model. The wheel force is then given by:

$$f_i^w = F_i^{ws} n_i^w \Lambda_i \qquad (2.26)$$

Using the tyre deflection rate $\dot{\delta}_i^w$, the tyre damping force $F_i^{wd}$ may be computed in a similar manner by using equations 2.1 to 2.6 and the prescribed tyre damping characterising parameters. The tyre damping force is then added to $f_i^w$ above to give the total tyre force on the specific axle $i$:

$$f_i^w = f_i^w + F_i^{wd} n_i^w \Lambda_i \qquad (2.27)$$

Limiting the tyre force to negative values, i.e. only compression allowed, the following rule is applied:

$$\text{If } f_i^w > 0 \text{ then set } f_i^w = 0 \qquad (2.28)$$

### 2.1.1.2 The spring, damper and bump stop forces

For each axle, $i$, the suspension deflection of the equivalent suspension is given by (refer to figure 2.5 for a schematic and section A2 of Appendix A):

$$\delta_i = \frac{c^y - (d_i^w + d_i + t_i \cos\beta_i)\sin\theta - w_i^y}{\cos\theta} - (h - r_i - \delta_i^t) \qquad (2.29)$$

and the deflection rate by direct differentiation with respect to time follows:

$$\dot{\delta}_i = \frac{\dot{q}_1}{\cos\theta} - (d_i^w + d_i + t_i \cos\beta_i)\dot{q}_2 - \frac{\dot{q}_{i+2}}{\cos\theta} \qquad (2.30)$$

In the equivalent suspension approach used in this study the actual springs, dampers and bump stops are modelled by the equivalent suspension as shown in figure 2.2. Due to the geometrical position of the actual spring on axle $i$, a ratio between the deflection of the actual spring and the equivalent suspension deflection $\delta_i$ exists. This ratio is given by $\kappa_i^s, i = 1,2,3,4$. Similarly for each axle $i$, a ratio between the actual damper and bump stops deflection and the equivalent suspension deflection exists. These ratios are respectively denoted by $\kappa_i^d$ and $\kappa_i^b, i = 1,2,3,4$.

The respective deflections may now be determined as follows. The deflection at the actual spring is given by:

$$\Delta_i^s = \delta_i \kappa_i^s + \delta_i^s \qquad (2.31)$$

where

$\kappa_i^s$ = the ratio between the actual spring deflection and that for the equivalent suspension,

$\delta_i^s$ = the initial spring deflection,

and the deflection at the actual bump stop:

$$\Delta_i^b = \delta_i \kappa_i^b + \delta_i^b \qquad (2.32)$$

where

$\kappa_i^b$ = the ratio between the actual bump stop deflection and that for the equivalent suspension,

$\delta_i^b$ = the initial bump stop deflection,

and the deflection rate at the actual damper:

$$\dot{\Delta}_i^d = \dot{\delta}_i \kappa_i^d \qquad (2.33)$$

where

$\kappa_i^d$ = the ratio between the actual damper deflection rate and that for the equivalent suspension.

Using the spring deflection $\Delta_i^s, i = 1,2,3,4,$ the spring force $F_i^s$ may be calculated using the spring stiffness versus deflection piece-wise data and equations 2.1 to 2.6. With the respective $F_i^s$ known, the equivalent suspension force due to the spring force may be obtained:

$$f_i^s = F_i^s n_i^s \kappa_i^s \tag{2.34}$$

where

$n_i^s$ = the number of springs on the axle.

Also at a deflection of $\Delta_i^b$ use the bump stop stiffness versus deflection piece-wise data and calculate the bump stop force $F_i^b$. Calculate the equivalent suspension force due to $F_i^b$:

$$f_i^b = F_i^b n_i^b \kappa_i^b \tag{2.35}$$

where

$n_i^b$ = the number of bump stops on the axle.

Similarly, using the damping coefficient versus deflection rate piece-wise data, the damper force $F_i^d$ may be determined at a specific deflection rate $\dot{\Delta}_i^d$. With $F_i^d$ known, the equivalent suspension force for axle $i$ may be calculated:

$$f_i^d = F_i^d n_i^d \kappa_i^d \tag{2.36}$$

where

$n_i^d$ = the number of dampers on the axle.

#### 2.1.1.3 Acceleration of the vehicle body

Once all the forces acting on the body are known the acceleration and pitch acceleration of the vehicle body can be computed.

From eq. 2.34 to 2.36 the total equivalent suspension force at each wheel $i$ is given by:

$$f_i^e = f_i^s + f_i^d + f_i^b \tag{2.37}$$

Applying a force equilibrium in the direction of the equivalent trailing arm (see figure 2.6) the force $f_i^a$ in each equivalent trailing arm is approximately given by (the effect of the acceleration of the axle in the direction of the trailing arm is neglected due to the fact that this acceleration will normally be small for $\beta_i \approx 180°$ and due to the fact that the mass of the axle $m_{i+1}$ is very small compared to $m_1$ ):

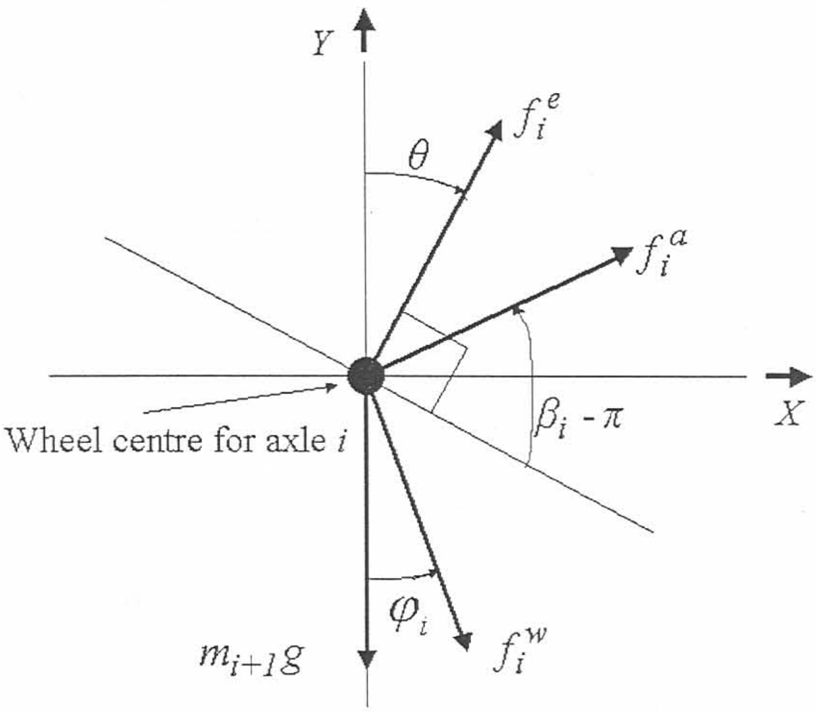


***Figure 2.6: Schematic of forces acting at the wheel centre***

$$f_i^a = -f_i^e \cos(\frac{3\pi}{2} - \beta_i) + f_i^w \cos(\frac{3\pi}{2} - \beta_i + \theta + \varphi_i) + m_{i+1} g \cos(\frac{3\pi}{2} - \beta_i + \theta) \qquad (2.38)$$

which simplifies to:

$$f_i^a = f_i^e \sin\beta_i + f_i^w \sin(\theta + \varphi_i - \beta_i) + m_{i+1} g \sin(\theta - \beta_i) \qquad (2.39)$$

The total sum of the components of the trailing arm forces in the direction of $q_1$ or Y in figure 2.7 is given by:

$$F^a = \sum_{i=1}^{4} f_i^a \cos(\frac{3\pi}{2} - \beta_i + \theta) = \sum_{i=1}^{4} f_i^a \sin(\theta - \beta_i) \qquad (2.40)$$

and the sum of the suspension forces:

$$F^s = \sum_{i=1}^{4} f_i^e \cos\theta \tag{2.41}$$

The body acceleration is now given by:

$$\ddot{q}_1 = \frac{-m_1 g - F^a - F^s}{m_1} \tag{2.42}$$

The moments acting on the vehicle body (refer to figures 2.3, 2.5 and 2.7 as well as the detailed derivation in section A3 of Appendix A) due to axle $i$ is given by:

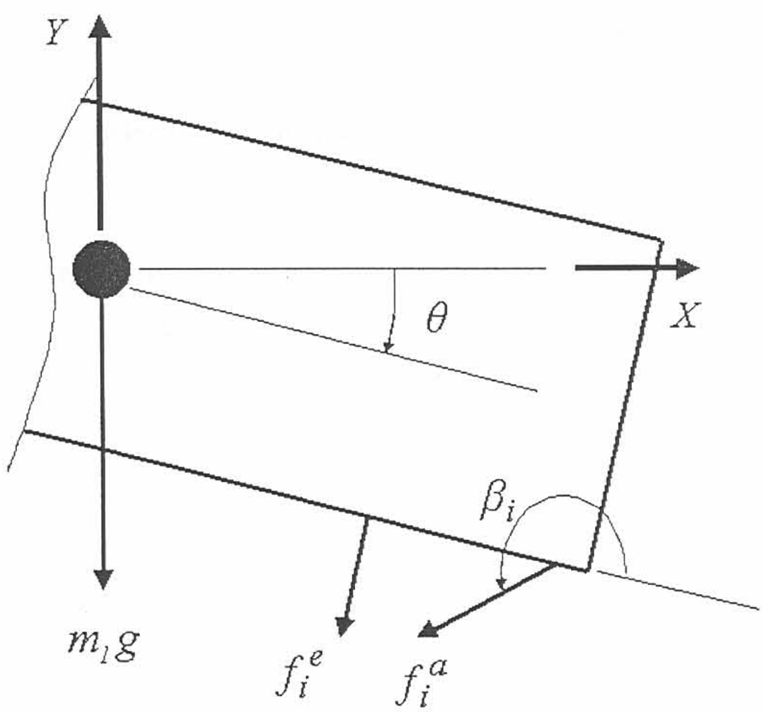


***Figure 2.7: Schematic of forces acting on vehicle body***

$$M_i = f_i^e(d_i^w + d_i + t_i \cos\beta_i) - f_i^a(d_i^w + d_i)\sin\beta_i - f_i^a(h - r_i - \delta_i^t - e_i)\cos\beta_i \tag{2.43}$$

The pitch acceleration can be determined from:

$$\ddot{q}_2 = \frac{\sum_{i=1}^{4} M_i}{I} \tag{2.44}$$

#### 2.1.1.4 Axle accelerations

The accelerations of the different wheels (perpendicular to the equivalent trailing arm) can be shown (see section A4 of Appendix A) to be given by:

$$\ddot{q}_i^a = \frac{-f_i^e \cos\beta_i + m_{i+1} g \cos(\beta_i - \theta) + f_i^w \cos(\beta_i - \theta - \varphi_i)}{m_{i+1}} \tag{2.45}$$

This acceleration can be transformed to the direction of the degrees of freedom for the axles as well as adding the acceleration of the equivalent trailing arm instantaneous centre to obtain the accelerations of the axle centres $i, i = 12,3,4$:

$$\ddot{q}_{i+2} = -\ddot{q}_i^a \cos(\beta_i - \theta) + \ddot{q}_1 - \ddot{q}_2 [(d_i^w + d_i)\cos\theta - (h - r_i - \delta_i^t - e_i)\sin\theta] \tag{2.46}$$

#### 2.1.1.5 Solving for the velocities and displacements

Equations 2.42, 2.44 and 2.46 represent a system of six second order differential equations. Once the initial conditions, i.e. initial displacements and velocities $q_i(0)$ and $\dot{q}_i(0), i = 1,2,...,6$ at $t = 0$ are specified, they may be solved numerically to give the displacements and velocities at successive time instants $t$ at intervals of $\delta^t$. In this study a fourth order Runga Kutta method [56] is use to solved the equations and the solution is initiated from equilibrium such that $\dot{q}_i(0) = 0$ for all $i$.

### 2.1.2 Equilibrium

Before applying the procedure described in 2.1.1 for the solution of the vehicle dynamics, it is important to first determine the initial equilibrium configuration of the vehicle system from which the solution is to be started. To obtain equilibrium at $t = 0$, the following heuristic iterative process is proposed and applied:

1. Set $q_i = \dot{q}_i = 0, \ i = 1,2,\ldots,6$ (2.47)
2. Determine the accelerations ($\ddot{q}_i$, $i = 1$ to $6$) using equations 2.42, 2.44 and 2.46.
3. For $i = 1,2,4,5,6$:

$$\begin{aligned} &\text{If } \ddot{q}_i > 0.005 \text{ then set } q_i = q_i + \ddot{q}_i / 5000 \\ &\text{If } \ddot{q}_i < -0.005 \text{ then set } q_i = q_i + \ddot{q}_i / 1330 \end{aligned} \tag{2.48}$$

4. And for $i = 2$:

$$\begin{aligned} &\text{If } \ddot{q}_i > 0.005 \text{ then } q_i = q_i + \ddot{q}_i / 10000 \\ &\text{If } \ddot{q}_i < -0.005 \text{ then } q_i = q_i + \ddot{q}_i / 1850 \end{aligned} \tag{2.49}$$

*(The values of 5000, 1330, 10000 and 1850 used in equations 2.48 and 2.49 were determined experimentally. The heuristic proved effective in obtaining equilibrium relatively quickly for most of the vehicle configurations tested.)*

5. Determine the sum of the absolute values of the vertical accelerations:

$$T^q = |\ddot{q}_1| + |\ddot{q}_3| + |\ddot{q}_4| + |\ddot{q}_5| + |\ddot{q}_6| \tag{2.50}$$

6. If $T^q < 0.005 + 0.005 * n_a$ and $|\ddot{q}_2| < 0.005$, where $n_a$ is the number of axles, then equilibrium is assumed, otherwise, with the current displacements $q_i$ again set $\dot{q}_i = 0, \ i = 1,2,\ldots,6$ and go to step 2.

Of course, in the event of failure of the above iterative scheme to produce equilibrium, the computationally more expensive option remains to perform the simulation with $v = 0$ until equilibrium is obtained. Analysing the results of the simulation will yield the required initial spring, bump stop and tyre deflections.

## 2.2 Optimisation algorithm

Mathematical optimisation is the process of the formulation and then the solution of a constrained optimisation problem of the general mathematical form:

$$\min imise_{\text{with respect to } x}\ f(x),\ \ x = (x_1, x_2, \ldots x_n) \in R^n \tag{2.51}$$

subject to constraints

$$g_j(x) <= 0,\ j = 1,2,\ldots.m \tag{2.52}$$

$$h_j(x) = 0,\ j = 1,2,\ldots..r < n \tag{2.53}$$

where $f(x)$, $g_j(x)$ and $h_j(x)$ are scalar functions of $x$ [53]. The variables $x$ are called the design variables, $f(x)$ the objective function and $g_j(x)$ *and* $h_j(x)$ are respectively referred to as the inequality and equality constraint functions.

The formulation of the optimisation problem requires identifying the objective function, the variables and the constraints. This is done by means of a mathematical model of the system or process that is to be optimised. The construction of an appropriate model, in this case of a vehicle suspension system, is thus the first step in the optimisation process. If the model is too simplistic, it will not give useful insight into the practical problem, but if it is too complex it may become difficult to solve [66]. Once the formulation has been done an optimisation algorithm can be selected to find the solution. Usually the algorithm and model are sufficiently complicated that a computer is needed to implement the optimisation process. There is no universal optimisation algorithm. Rather, there are numerous algorithms, each of which is tailored to a particular type of optimisation problem.

Excellent texts on design optimisation exist, including in particular those of Arora [68], Haftka & Gürdal [69], Papalambros & Wilde [70] and Vanderplaats [71]. These works describe various classical and traditional optimisation algorithms that have been used with success in solving engineering optimisation problems. In this study, however, the relatively novel LFOPC algorithm of Snyman [53-55] is selected as the optimisation algorithm to be used. Section A5 of Appendix A gives a more detailed description of the LFOPC algorithm. The LFOPC algorithm has the following characteristics:

i. it uses only function gradient information,
ii. no explicit line searches are performed,
iii. it is extremely robust and handles steep valleys and discontinuities in functions and gradients with ease,

iv. the algorithm seeks relative low local minima and can thus be used as a basic component in a methodology for global optimisation,
v. it is not as efficient on smooth and near quadratic functions as classical methods, but
vi. it is particularly robust and reliable in dealing with the presence of numerical noise in the objective and constraint functions – this is expected to be the case in this study where the objective function is to be evaluated via numerical simulations.

For a complete description of the LFOPC mathematical code the reader is referred to [51, 53-55].

In using the LFOPC optimisation algorithm in conjunction with the vehicle simulation program for the optimisation of vehicle and/or suspension characteristics, the following demands are to be satisfied:

i. A baseline vehicle is to be modelled.
ii. The user should be able to select the required vehicle parameters to be optimised and couple them to design variables of the optimisation code. For a specific vehicle parameter selected the baseline design variable value is to be normalised to a value of 1, i.e. when the design variables are changed by the LFOPC algorithm then:

$$\textit{New vehicle parameter} = \textit{Baseline vehicle parameter} * \textit{design variable} \qquad (2.54)$$

iii. Constraints and general parameters for the optimisation process are to be prescribed.
iv. The user should be able to select / construct a specific suitable objective function to be minimised.
v. The vehicle dynamic simulation is to be performed for the specified set of vehicle parameters with the results of the simulation being stored.
vi. Using the saved simulation results the specific objective function is to be calculated.
vii. The LFOPC algorithm should be capable of communicating with the simulator so that the effect on the objective function, of small changes in the respective values of the design variables, can be determined. In particular this is necessary for the computation of approximations to the components of the gradient vector of the objective function through forward finite differences.
viii. Using the gradient vector the optimisation algorithm should compute a next set of design variables lying along a trajectory leading to the optimum design. Thus each new set of design variables represents the next step (iteration) along the optimisation path.
ix. At each iteration the whole process (step v to viii) is to be repeated until no further significant improvement in the objective function is obtained. The final set of design variables is taken as the optimum giving a corresponding optimum objective function value.

Etman [23] states that the coupling of a detailed and comprehensive multi-body code to a mathematical programming algorithm may be difficult to implement and can lead to high computational cost. In heeding this warning an attempt is made in this study to keep the vehicle model as simple as possible. The dramatic increase in computer processing speed over the past few years has also made the development of a realistic suspension optimisation system, by means of which the above demands may be met, a more realistic proposition.

## 2.3 Summary

In this chapter the mathematical model for the two dimensional simulation of vehicle dynamics is described. The respective six piece-wise continuous linear approximations used to describe the non-linear suspension characteristics of the springs, dampers, bump stops and tyres to be used in the simulation, are also given. Basically the vehicle model consists of up to five solid bodies, one corresponding to the vehicle body and the others to up to four axles on the vehicle. Six degrees of freedom describe the motion of the system of bodies. The suspension is modelled by using an equivalent trailing arm approach. The governing equations of motion of the system are derived. Accelerations are determined once the forces acting on the bodies due to prescribed road input are calculated. Using a fourth order Runga Kutta numerical integration scheme the velocities and displacements of the bodies are computed. The importance of determining the equilibrium configuration of the vehicle before commencing the simulation is stressed. The actual method by means of which the required equilibrium configuration is determined through iteration is briefly described.

The coupling of the LFOPC optimisation algorithm to the vehicle dynamics model is also briefly discussed. Using the LFOPC algorithm a set of design variables, related to vehicle parameters, can be specified. The optimum set with respect to a user defined objective function may then be determined by LFOPC.

Although the literature overview warns of the difficulties associated with coupling a multi-body code directly to a mathematical optimisation algorithm, this approach is nevertheless taken in this study. Due to the fact that computer processing power and speed has recently increased dramatically such a task has become more realisable. Keeping the multi-body code as simple as possible and exploiting the robustness and effectiveness of the LFOPC algorithm, an attempt is now made to develop a practically useful suspension optimisation system.